Chen et al. BMC Pulmonary Medicine (2024) 24:249
https://doi.org/10.1186/s12890-024-03061-2

BMC Pulmonary Medicine

RESEARCH Open Access

Continuous estimation of respiratory system compliance and airway resistance during pressure-controlled ventilation without end-inspiration occlusion

Yuqing Chen[1*], Yueyang Yuan[2], Qing Chang[1], Hai Zhang[1], Feng Li[1] and Zhaohui Chen[3]

Abstract

Background Assessing mechanical properties of the respiratory system (C_{st}) during mechanical ventilation necessitates an end-inspiration flow of zero, which requires an end-inspiratory occlusion maneuver. This lung model study aimed to observe the effect of airflow obstruction on the accuracy of respiratory mechanical properties during pressure-controlled ventilation (PCV) by analyzing dynamic signals.

Methods A Hamilton C3 ventilator was attached to a lung simulator that mimics lung mechanics in healthy, acute respiratory distress syndrome (ARDS) and chronic obstructive pulmonary disease (COPD) models. PCV and volume-controlled ventilation (VCV) were applied with tidal volume (V_T) values of 5.0, 7.0, and 10.0 ml/kg. Performance characteristics and respiratory mechanics were assessed and were calibrated by virtual extrapolation using expiratory time constant (RC_{exp}).

Results During PCV ventilation, drive pressure (DP) was significantly increased in the ARDS model. Peak inspiratory flow (PIF) and peak expiratory flow (PEF) gradually declined with increasing severity of airflow obstruction, while DP, end-inspiration flow (EIF), and inspiratory cycling ratio (EIF/PIF%) increased. Similar estimated values of C_{rs} and airway resistance (R_{aw}) during PCV and VCV ventilation were obtained in healthy adult and mild obstructive models, and the calculated errors did not exceed 5%. An underestimation of C_{rs} and an overestimation of R_{aw} were observed in the severe obstruction model.

Conclusion Using the modified dynamic signal analysis approach, respiratory system properties (C_{rs} and R_{aw}) could be accurately estimated in patients with non-severe airflow obstruction in the PCV mode.

Keywords Pressure-controlled ventilation, Compliance, Airway resistance, Simulation, Chronic obstructive pulmonary disease

*Correspondence:
Yuqing Chen
chenyqn1969@126.com
[1]Department of Respiratory Medicine, Shanghai Chest Hospital, Shanghai Jiao Tong University, No.241, West Huaihai Road, Shanghai 200030, China
[2]School of Mechanical and Electrical Engineering, Hunan City University, Yiyang 413099, China
[3]College of Information Technology, Shanghai Jian Qiao University, Shanghai 201306, China

Background

Mechanical ventilation is an important lifesaving procedure with wide clinical applications for various critical conditions. The adequate setting of ventilator parameters should be based on the patient's condition for optimal patient outcomes and to minimize ventilator-associated injury and complications [1, 2]. Pressure-controlled ventilation (PCV) is broadly used for cases of severe respiratory failure. PCV improves arterial oxygenation and decreases peak airway pressure because it decelerates inspiratory low. However, PCV has some limitations, including insufficient ventilation and excessive ventilation [3–8].

Currently, the dynamic properties of the respiratory system and engineering models for various diseases are exploited in the diagnosis and treatment of pulmonary disorders [9, 10]. However, mechanical features cannot be assessed directly during mechanical ventilation and are commonly presented as lumped indicators, including airway resistance (R_{aw}) and compliance (C_{rs}) [11, 12]. Static compliance (C_{st}) is an important physiological index for evaluating the elastic properties of the overall respiratory system in invasive cases and is calculated by the ratio of the tidal volume to driving pressure [13]. C_{st} can be monitored by setting an end-inspiratory occlusion in the volume-controlled ventilation (VCV) mode. During PCV, an appropriate inspiratory time should be preset to acquire the approximate plateau pressure (P_{plat}). Nevertheless, setting an appropriate inspiratory time may be challenging because the patient's condition may change quickly. In addition, end-inspiration occlusion necessitates ventilation to be discontinued. Furthermore, this maneuver can be influenced by strong, spontaneous breathing. Therefore, other methods that do not require end-inspiratory occlusion need to be developed [14, 15].

Recently, methods have been proposed for the assessment of respiratory system properties without end-inspiration occlusion. Multiple linear regression (MLR), considering the least-squares fitting (LSF) technique, constitutes the most applied tool in recent years. It approximates C_{st} and R_{aw} with high accuracy in case of negligible spontaneous breathing effort [16–18]. Further tools encompass the constrained optimization strategy [19], electrical impedance tomography (EIT) monitoring, linear fitting of the flow velocity waveform, short expiratory occlusions, repeated changes in pressure support level, and artificial neural networks [20–23]. Still, the above techniques have some limitations: some do not adapt to spontaneous breathing conditions [16–18], while others apply sophisticated medical information or specific manual maneuvers, and others use empirical parameters [20, 22]. More importantly, most of them have more accurate measurements during VCV with constant inspiratory flow, with reduced accuracy when inspiratory flow is variable, such as in the PCV and PSV modes or spontaneous breathing effort. Secondly, the noise interference of ventilation waveforms exists in the real clinical setting, and noises encompass spontaneous breathing efforts, suctions, and coughing. Selecting adequate breaths that are less affected by noise might enhance accuracy in C_{st} and R_{aw} estimations.

In mechanically ventilated cases, expiration is a passive process depending on the expiratory time constant (RC_{exp}) of the respiratory system. RC_{exp} reflects the mechanical features of the respiratory system [elastance and resistance ($RC_{exp} = R_{aw} \times C_{rs}$)] and reveals the changes in the features of the pneumatic respiratory system [24]. C_{rs} and R_{aw} might be obtained from the passive deflation of lungs by using RC_{exp} and specific equations. In a previous bench study by the authors, the C_{rs} value was generally overestimated in the active breathing patient and underestimated in severe obstructive conditions, and the estimated error of R_{aw} by the RC_{exp} technique was minimal during passive breathing [15]. Recently, respiratory mechanics were estimated by modifying ventilation waveforms in the PCV mode to assess C_{st} and R_{aw} obtained by the end-inspiratory occlusion maneuver in the VCV mode. The continuous ventilation waveforms were examined, and an extra virtual tidal volume (V_T) was calculated using RC_{exp} and an appropriate equation. Then, respiratory mechanics were estimated by analyzing the dynamic signals, which considerably improved static measurements. Such an approach improves estimation precision in respiratory system mechanics via real-time collection of respiratory data from the inspiration and expiration phases by applying specific Eqs. [25, 26]. C_{st} and R_{aw} measurements based on the end-inspiratory occlusion maneuver in the real clinical setting were considered the gold standard for the validation of the proposed approach. The present study aimed to assess the accuracy of respiratory mechanical properties by the extra virtual V_T in the PCV mode.

Methods

Lung models

The ASL 5000 Breathing Simulator (IngMar Medical, Pittsburg, PA, USA) features a computerized lung simulator with a piston that moves in a cylinder. This simulator was set to a single compartment based on a work by Beloncle et al. and previous bench studies by the authors [15, 27]. The applied respiratory mechanics parameters simulated an adult patient (65 to 70 kg body weight) placed in the semi-recumbent position. Six clinical scenarios with/without expiratory flow limitation (EFL) were constructed as follows [10, 28, 29]: healthy adult [inspiratory resistance (R_{insp}) and expiratory resistance (R_{exp}) of 5.0 $cmH_2O/L/s$], mildly, moderate-to-severe obstruction [R_{insp}=R_{exp}=10.0, 15.0, and 20.0 $cmH_2O/L/s$], severe obstruction with EFL [R_{insp}=10.0 $cmH_2O/(L/s)$, R_{exp}=20.0 $cmH_2O/L/s$], and ARDS [R_{insp}=R_{exp}=10 $cmH_2O/L/s$]. C_{st} was set at 30 (ARDS) and 60 (COPD) mL/cmH_2O, and inspiratory time at 0.8 s (ARDS) and 1.6 s (COPD). Inspired oxygen fraction (F_IO_2) was 0.21 for all measurements.

Ventilator settings

A dry circuit was used for the bench work, simulating a passive condition with both breathing frequency and P_{mus} of zero. A Hamilton C3 ventilator (Hamilton Medical AG, Bonaduz, Switzerland) was attached to the lung simulator calibrated by the end-inspiratory occlusion maneuver in the VCV mode utilizing a constant flow. The Hamilton C3 device was used in the VCV mode. Positive end-expiratory pressure (PEEP) was 5.0 cmH_2O, and the backup breathing rate was 10 breaths/min. During VCV and PCV, respiratory mechanics setting was performed to maintain the output tidal volume (V_T) at 5.0, 7.0, and 10.0 ml/kg. A reduced inspiratory rise time was applied to prevent overshooting in the PCV mode.

Data collection

After baseline pressure stabilization, typical breaths were selected and recorded at 1-min intervals. Data were obtained for a total of six times after inspiratory pressure levels were adjusted in each lung model. All breaths were assessed offline using the ASL 5000 breathing simulator software.

Peak inspiratory flow (PIF), end-inspiratory flow (EIF), end-inspiratory pressure (EIP), and actual inspiratory time (T_I) were determined using the simulator. Expiratory V_T was also evaluated. Peak expiratory flow (PEF) and total PEEP were collected in the expiration phase (Figure S1).

Respiratory mechanics indexes were considered the main determinants of the interaction between the patient and the ventilator. During PCV, the quasi-static two-point compliance of the respiratory system (C_{rs}) was determined as V_T by driving pressure (DP). DP was the difference between EIP and total PEEP obtained at end-inspiration and end-expiration, respectively. RC_{exp} was the V_T/flow ratio at 75% of expiratory V_T [30]. The equations representing these relationships are:

Extra virtual tidal volume:

$$V_{T\,virtual} = RC_{exp} \times EIF \tag{1}$$

$$C_{rs} = (V_{TE} + V_{T\,virtual}) / (EIP - PEEP) \tag{2}$$

Inspiratory resistance (R_{insp}) was derived from the following equations considering dynamic signals:

$$P_{Ers\,insp} = (V_{TE} - V_{PIF}) / C_{rs} \tag{3}$$

$$R_{insp} = [P_{PIF} - (EIP - P_{Ers\,insp})] / PIF \tag{4}$$

Expiratory resistance (R_{exp}) was assessed with Eqs. 5 and 6:

$$P_{Ers\,exp} = (V_{TE} - V_{PEF}) / C_{rs} \tag{5}$$

$$R_{exp} = [P_{PEF} - (EIP - P_{Ers\,exp})] / PEF \tag{6}$$

The percentages of measurement errors for compliance or resistance (%error C_{rs} and %error R_{aw}) were calculated as follows [27]:

$$\%\,error\ C_{rs} = (C_{rs-estimate} - C_{rs-VCV}) / C_{rs-VCV} \times 100\% \tag{7}$$

$$\%\,error\ R_{aw} = (R_{aw-estimate} - R_{aw-VCV}) / R_{aw-VCV} \times 100\% \tag{8}$$

Statistical analysis

All analyses were performed using SPSS 19.0 (IBM, Armonk, NY, USA). Data were shown as means±standard deviations (SDs). The Shapiro-Wilk test was used for normality assessment. One-way ANOVA was used for comparisons in different settings. C_{rs}, R_{insp}, and R_{exp} were calculated in the VCV mode using the end-inspiration occlusion approach and the dynamic signal analysis method with extra virtual V_T in the PCV mode, with a two-tailed *t*-test for comparisons. Absolute differences between the extra virtual V_T and occlusion methods were determined, and $P<0.01$ indicated statistical significance. Differences between PCV and VCV were determined as absolute percentages of values measured in the VCV mode.

Results

EIF and extra virtual V_T in the PCV mode under passive breathing

In PCV, EIF/PIF% was not above 5% in the non-severe obstructive lung models [R_{aw} ≤10.0 $cmH_2O/L/s$] and close to 0 in the ARDS lung model. EIF/PIF% was increased with the aggravation of airflow obstruction, i.e., about 10% at a R_{aw} of 20.0 $cmH_2O/L/s$ ($P<0.001$). Extra virtual V_T and the percentage of extra virtual V_T and V_{TE} (ΔV_T%) were also increased (all $P<0.05$). Compared with the normal adult lung model, there were significant differences in EIF/PIF% and ΔV_T% under moderate to severe obstructive conditions (Table 1).

Estimation of C_{rs} in various models in the VCV and PCV modes

Inspiratory V_T in the PCV mode was corrected by RC_{exp} and EIF. The estimated value of C_{rs} was larger than the value without extra virtual V_T calibration and close to the value obtained in the VCV mode with end-inspiratory

Table 1 EIF/PIF% and ΔV_T% in various lung models in the PCV mode

	Normal adult (C_{rs}=60, R_{insp}=R_{exp}=5.0)	**Mild obstructive (C_{rs}=60, R_{insp}=R_{exp}=10.0)**	**Moderate obstructive (C_{rs}=60, R_{insp}=R_{exp}=15.0)**	**Severe obstructive (C_{rs}=60, R_{insp}=R_{exp}=20.0)**	**Obstructive with EFL (C_{rs}=60, R_{insp}=10.0, R_{exp}=20.0)**	**ARDS (C_{rs}=30, R_{insp}=R_{exp}=10.0)**
EIF/PIF%	1.34 ± 0.42	1.74 ± 0.86 (t = 1.7732) (P = 0.0426)	5.55 ± 0.65* (t = 23.0803) (P < 0.001)	10.86 ± 0.41* (t = 68.8143) (P < 0.001)	1.80 ± 0.48* (t = 3.0599) (P = 0.0022)	0.16 ± 0.20* (t = 10.7619) (P < 0.001)
ΔV_T>%	1.12 ± 0.33	1.58 ± 0.75 (t = 2.3818) (P = 0.0115)	4.66 ± 0.61* (t = 21.6554) (P < 0.001)	10.07 ± 0.61* (t = 54.7503) (P < 0.001)	1.67 ± 0.77* (t = 2.7854) (P = 0.0043)	0.13 ± 0.16* (t = 11.4528) (P < 0.001)

*P value (Student's t-test) for comparing normal adult and airflow obstruction lung models. Data are mean ± standard deviation, from 18 measurements/cases

Table 2 System compliance (C_{rs}) among lung models in different ventilatory modes

	Normal adult (C_{rs}=60, R_{insp}=R_{exp}=5.0)	**Mild obstructive (C_{rs}=60, R_{insp}=R_{exp}=10.0)**	**Moderate obstructive (C_{rs}=60, R_{insp}=R_{exp}=15.0)**	**Severe obstructive (C_{rs}=60, R_{insp}=R_{exp}=20.0)**	**Obstructive with EFL (C_{rs}=60, R_{insp}=10.0, R_{exp}=20.0)**	**ARDS (C_{rs}=30, R_{insp}=R_{exp}=10.0)**
VCV	60.37 ± 0.65	59.93 ± 0.74	59.24 ± 2.06	57.38 ± 1.00	56.17 ± 1.23	30.16 ± 0.24
PCV	58.99 ± 0.60	58.37 ± 0.83	54.62 ± 1.15	49.28 ± 0.34	52.79 ± 1.02	29.97 ± 0.20
PCV-cal	59.92 ± 0.66* (t = 2.0610) (P = 0.047)	59.03 ± 0.84	57.16 ± 1.25	54.24 ± 0.30	53.67 ± 1.04	30.01 ± 0.19* (t = 2.0790) (P = 0.045)
F	21.96	17.05	40.56	747.05	45.68	18.59
P	< 0.01	< 0.01	< 0.01	< 0.01	< 0.01	< 0.01

occlusion. The estimated C_{rs} decreased significantly with increasing severity of airflow obstruction in either ventilatory mode, and uncalibrated C_{rs} values were only 49.28±0.34 mL/cmH_2O (PCV mode) and 57.38±1.00 mL/cmH_2O (VCV mode) (P<0.01) in the severe obstructive lung model [R_{aw}=20.0 cmH_2O/L/s]. After the correction of extra virtual V_T, the calculated errors were <5% in all four lung models [R_{aw}≤15.0 cmH_2O/L/s], which showed no significant differences compared with estimated values in the VCV mode (Table 2; Fig. 1A).

Estimation of R_{aw} in various models in the VCV and PCV modes

There were similar estimated R_{insp} and R_{exp} in the PCV and VCV modes with R_{aw} ≤10.0 cmH_2O/L/s, and calculated errors were ≤10.0%. After V_T calibration, the estimated errors of R_{insp} and R_{exp} were reduced to <5%. In severe obstructive and obstructive with EFL models, the estimated errors of R_{insp} and R_{exp} were significantly reduced and were below 10% after V_T calibration (Tables 3 and 4; Fig. 1B and C).

Bland-Altman analysis of differences between the PCV and VCV modes

In all five lung profiles with normal system compliance (60.0 mL/cmH_2O), the difference in C_{rs} between the V_T calibration and end-inspiration occlusion approaches was 1.82±1.43 mL/cmH_2O; the weighted correlation coefficient of C_{rs} equaled 0.549 after V_T calibration (P<0.001). The differences of R_{insp} and R_{exp} values in all lung models were 0.79±1.96×0.89 and 0.38±1.96×0.69 cmH_2O/L/s, and the weighted correlation coefficients of R_{insp} and R_{exp} were equal to 0.954 and 0.969, respectively (all P<0.001) (Figs. 2 and 3).

Discussion

This bench study mostly revealed the following. (1) During PCV under the passive breathing condition, the estimated error was affected by the severity of airway obstruction, significantly underestimated in C_{rs}, and significantly overestimated in R_{aw} without V_T calibration. (2) In the non-severe obstructive condition [R_{aw} ≤ 10.0 cmH_2O/L/s], estimated errors were ≤10% in calculated C_{rs} and R_{aw}. (3) The estimated accuracies of C_{rs}, R_{insp}, and R_{exp} were improved by V_T calibration with extra virtual inspiratory volume.

During mechanical ventilation, assessing the respiratory mechanics by end-inspiratory occlusion with a constant inspiratory flow is a classic measurement method. However, the occlusion technique may be performed with no gas flow and fixed tidal volume. It is important for the patient to make no efforts during static measurements, whether related to disease, sedation, or paralysis, and special ventilatory settings are also required (such as constant inspiratory flow and end-inspiration pause) [31–33]. The most important concern is that measurement data are reflected by mechanical properties under static or quasi-static conditions. The occlusion method could neither be adapted to the PCV mode since inspiratory flow is always variable nor be used in assisted

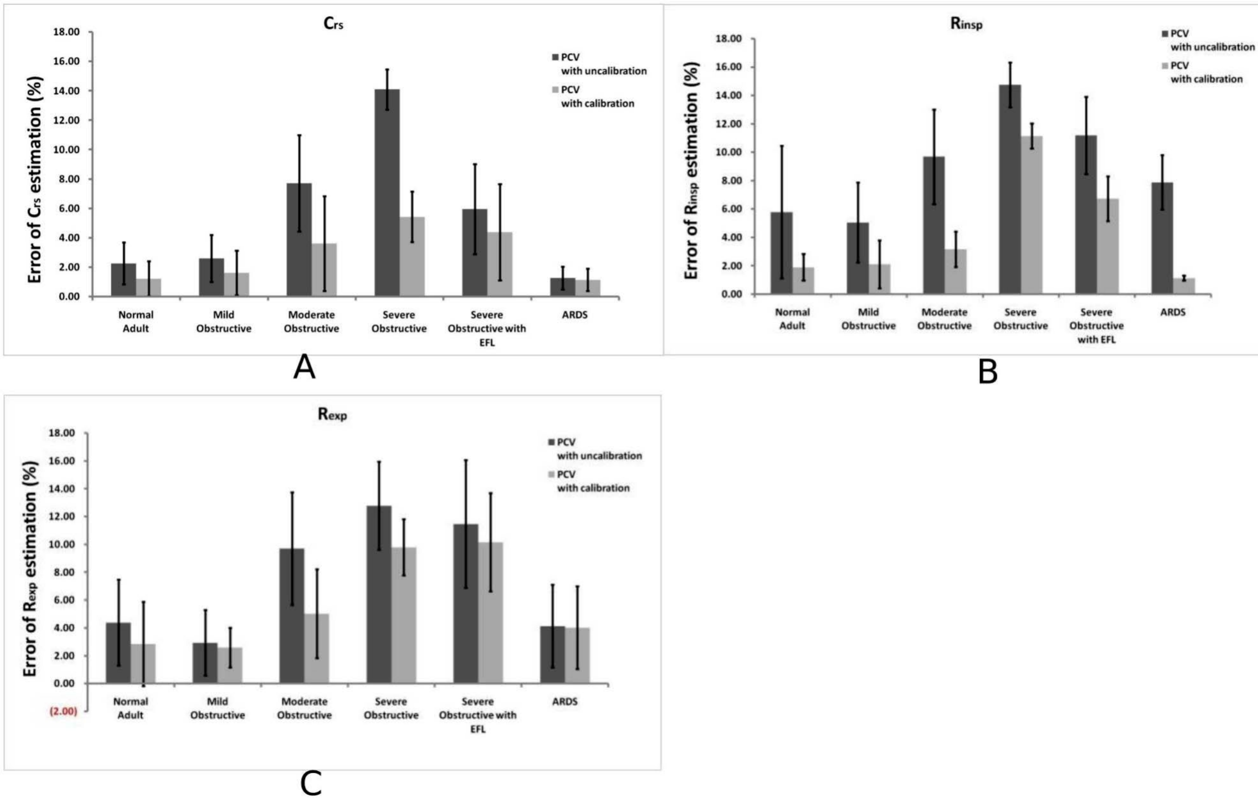

Fig. 1 **(A)** Errors of system compliance (Crs) in various lung models during PC ventilation. **(B)** Errors of Rinsp in different lung models during PC ventilation. **(C)** Errors of Rexp in different lung models during PC ventilation. Data are shown as mean ± SD

Table 3 Comparison of R_{insp} between lung models in different ventilatory modes

	Normal adult (C_{rs}=60, R_{insp}=R_{exp}=5.0)	**Mild obstructive (C_{rs}=60, R_{insp}=R_{exp}=10.0)**	**Moderate obstructive (C_{rs}=60, R_{insp}=R_{exp}=15.0)**	**Severe obstructive (C_{rs}=60, R_{insp}=R_{exp}=20.0)**	**Obstructive with EFL (C_{rs}=60, R_{insp}=10.0, R_{exp}=20.0)**	**ARDS (C_{rs}=30, R_{insp}=R_{exp}=10.0)**
VCV	5.05 ± 0.28	10.04 ± 0.25	14.93 ± 0.41	19.68 ± 0.37	10.25 ± 0.38	10.54 ± 1.02
PCV	5.27 ± 0.15	10.53 ± 0.39	16.31 ± 0.39	22.57 ± 0.81	11.38 ± 0.32	10.10 ± 0.33
PCV-cal	5.18 ± 0.14* (t = 1.7618) (P = 0.087)	10.72 ± 0.51	15.78 ± 0.43	22.38 ± 0.71	12.07 ± 0.43	10.09 ± 0.34* (t = 1.7757) (P = 0.085)
F	5.48	14.00	51.81	108.78	105.60	2.82
P	0.007	< 0.01	< 0.01	< 0.01	< 0.01	0.069

*P-values (Student t-test) are for comparisons between the VCV and PCV modes. Data are shown as means ± standard deviations and are the results of 18 measurements/cases

Table 4 R_{exp} values in lung models in different ventilatory modes

	Normal adult (C_{rs}=60, R_{insp}=R_{exp}=5.0)	**Mild obstructive (C_{rs}=60, R_{insp}=R_{exp}=10.0)**	**Moderate obstructive (C_{rs}=60, R_{insp}=R_{exp}=15.0)**	**Severe obstructive (C_{rs}=60, R_{insp}=R_{exp}=20.0)**	**Obstructive with EFL (C_{rs}=60, R_{insp}=10.0, R_{exp}=20.0)**	**ARDS (C_{rs}=30, R_{insp}=R_{exp}=10.0)**
VCV	5.38 ± 0.18	10.35 ± 0.22	14.69 ± 0.77	19.93 ± 0.47	19.44 ± 1.13	10.18 ± 0.29
PCV	5.57 ± 0.13	10.59 ± 0.59	16.08 ± 0.31	22.47 ± 0.41	20.48 ± 0.84	10.48 ± 0.28
PCV-cal	5.41 ± 0.15* (t = 0.5432) (P = 0.587)	10.42 ± 0.29* (t = 0.8159) (P = 0.420)	15.12 ± 0.26* (t = 2.2448) (P = 0.0314)	21.77 ± 0.36	20.06 ± 0.80* (t = 1.8999) (P = 0.066)	10.36 ± 0.28* (t = 1.8944) (P = 0.0667)
F	7.85	1.71	36.15	179.22	5.64	5.11
P	0.0011	0.1908	< 0.01	< 0.01	0.0061	0.0095

*P values (Student's t-test) are for comparisons between the VCV and PCV. Data are mean ± standard deviation from 18 measurements/cases

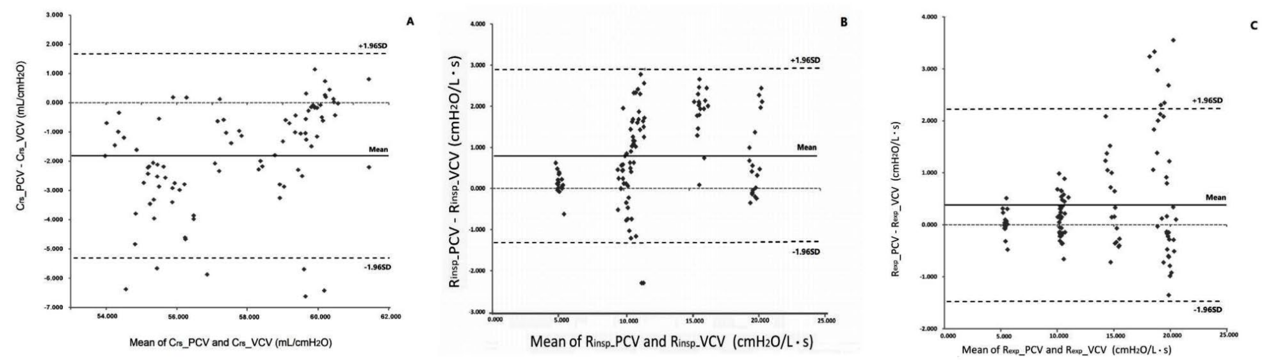

Fig. 2 Bland-Altman plots depicting system compliance (**A**), inspiratory resistance (**B**) and expiratory resistance (**C**) by the V_T calibration and end-inspiration occlusion approaches. Data from 5 (C_{rs}) and 6 (R_{aw}) lung models, in totally 168 breaths. Each circle reflects one breath for a given model. Dashed lines in the middle depict mean differences between the V_T calibration and end-inspiration occlusion approaches. The remaining two dashed lines are mean ± 1.96*SD

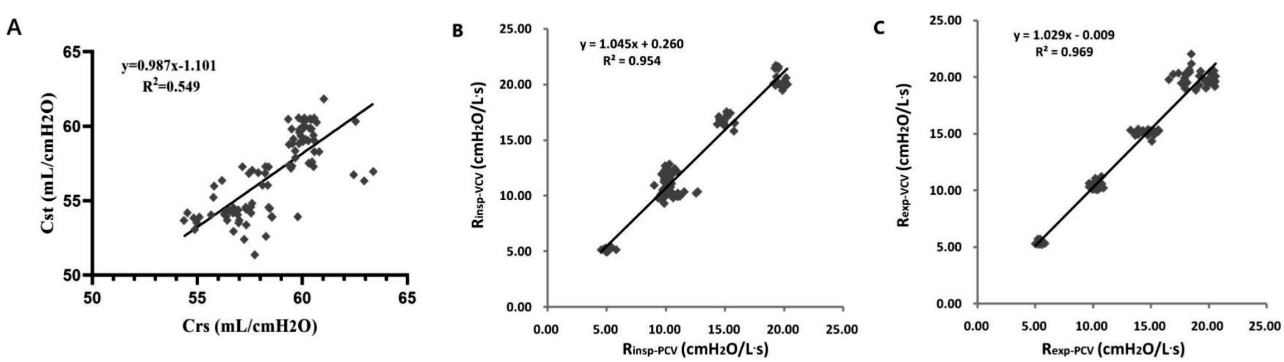

Fig. 3 Associations of estimated C_{rs} (**A**), R_{insp} (**B**) and R_{exp} (**C**) with gold standard obtained by the end-inspiration occlusion approach. Data from 5 (C_{rs}) and 6 (R_{aw}) lung models, totally 168 breaths were examined. Each circle reflects one breath for a given model

ventilation in which the spontaneous effort is always present and variable. Recently, several continuous respiratory mechanics measurement techniques, including LSF and expiratory time constant method (RC_{exp}), have been developed. These newer approaches not only have good adaptability and anti-noise-interference performance but also could be applied during assisted mechanical ventilation with spontaneous breathing [34].

Volta et al. found that EFL substantially reduces the accuracy of resistance and compliance assessed by the LSF method; the determination of respiratory indexes during inspiration helps evaluate respiratory mechanics in flow-limited COPD cases, and the LSF technique could detect $PEEPi_{dyn}$ only using inspiratory data [18]. However, the estimated error of LSF was affected by the spontaneous breathing effort, and Raw underestimation and C_{rs} overestimation were observed in the PSV mode [16, 35]. The other approaches have certain limitations. Some could not deal with significant spontaneous breathing, while others are based on sophisticated medical equipment or manual maneuvers, preventing their routine clinical use [18–22]. Recently, Pan et al. proposed a tool measuring quasi-static respiratory system compliance (C_{q-stat}) in the PCV mode without the need for the end-inspiratory occlusion maneuver, with a virtual assessment of flow-time waveforms with end-inspiration flow not equaling zero, to allow for C_{q-stat} determination [14]. In this bench study, the dynamic signal analysis approach was used to collect and calculate gas flow, airway pressure, and volume data at different time points during mechanical ventilation, and the estimated C_{rs}, R_{insp}, and R_{exp} were calibrated by virtual extrapolation of V_T when end-inspiration flow was not zero. Dynamic signal analysis does not require special maneuvers such as long-time pauses at the inspiration or expiration phase [26]. In healthy adults and mild obstruction lung models, no significant differences were found in estimated C_{rs} and R_{aw} (R_{insp} and R_{exp}) between the PCV and VCV modes with EIF < 2.0 L/min and EIF/PIF% < 5.0%. The calculated error was increased when EIF/PIF% was above 5% in the PCV mode. Due to the exacerbation of airflow obstruction, PIF was decreased, and EIF did not drop to zero at the end of inspiration. EIF/PIF% was increased to about 10%, resulting in V_T decrease, C_{rs} underestimation, and

R_{aw} overestimation. After V_T calibration with RC_{exp} and EIF, the accuracy of the estimation was improved significantly, and the values obtained were similar to those estimated in the VCV mode by the occlusion method.

In the classic system compliance (C_{rs}) calculation equation, C_{rs} is the ratio of the monitored tidal volume (V_T) to the driving pressure (DP) of the airway. The tidal volume is the sum of the gas output capacity of the ventilator during the inhalation phase. In the classic calculation scheme, the tidal volume is the gas output capacity value measured after the end-inspiratory flow rate reaches 0. On the other hand, in this study, due to the special nature of the PCV mode, the end-inspiratory flow rate does not always decrease to 0. Therefore, an additional parameter (i.e., the extra virtual tidal volume) was designed to simulate the gas capacity generated after the flow rate continued to decrease to 0. It was found that the addition of the extra virtual tidal volume was of great significance for calculating C_{rs} under the PCV ventilation state.

One of the limitations of the present bench study is the standardization of simulation indexes for the respiratory system's mechanics in the lung model. Although the mechanical lung simulator cannot completely replace animal experiments and real clinical practice, the ASL 5000 mechanical lung simulator also has its unique advantages. Firstly, it can simulate simple single-chamber linear models and complex lung mechanics models with dual-chamber nonlinearity. In this study, we attempted to explore a new respiratory mechanics calculation scheme that can be applied to non-interrupted breathing and non-constant inspiratory flow mechanical ventilation conditions and can accurately calculate the respiratory mechanics characteristics of patients with different respiratory system diseases. Therefore, a mechanical lung simulator was first used for the experiment because its output data is relatively stable, and this lung simulator is also often selected in many mechanical simulation experiments. Further animal experiments will be conducted in the future [36]. Secondly, the passive breathing condition was simulated during PCV since spontaneous breathing effort might affect V_T and C_{rs}. It is not clear whether this scheme could be applied to other assisted ventilatory modes such as PSV. Thirdly, airway resistance varies with gas flow through the trachea and bronchus. Therefore, the above data reflect maximal resistance in a patient during breathing, and whether they can be translated in the clinical setting is unknown. Therefore, further clinical trials are warranted.

Conclusion

Using the modified dynamic signal analysis approach, respiratory system properties (C_{rs} and R_{aw}) could be accurately estimated in patients with non-severe airflow obstruction in the PCV mode. Compared with the VCV mode with constant flow, inspiratory flow decreased exponentially in the PCV mode. PIF and the deceleration rate of inspiratory flow were dependent upon the mechanical characteristics of the respiratory system, especially airflow obstruction.

Abbreviations

PCV	Pressure-controlled ventilation
COPD	Chronic obstructive pulmonary disease
VCV	Volume-controlled ventilation
V_T	Tidal volume
DP	Drive pressure
PIF	Peak inspiratory flow
PEF	Peak expiratory flow
EIF	End-inspiration flow
EIF/PIF%	Inspiratory cycling ratio
R_{aw}	Airway resistance
C_{st}	Static compliance
P_{plat}	Plateau pressure
MLR	Multiple linear regression
LSF	Least-squares fitting
EIT	Electrical impedance tomography
RC_{exp}	Expiratory time constant
EFL	Expiratory flow limitation
PEEP	Positive end-expiratory pressure
EIP	End-inspiration pressure
T_I	Inspiratory time
C_{rs}	Respiratory system compliance
DP	Driving pressure
SD	Standard deviation
C_{q-stat}	Quasi-static respiratory system compliance

Supplementary Information

The online version contains supplementary material available at https://doi.org/10.1186/s12890-024-03061-2.

Supplementary Material 1

Supplementary Material 2

Acknowledgements
Not applicable.

Author contributions
Yuqing Chen and Feng Li contributed to the concept and drafted the manuscript or substantively revised it. Yueyang Yuan contributed to the manuscript design. Qing Chang, Hai Zhang, and Zhaohui Chen contributed to data acquisition and analysis. FL contributed to the interpretation of the data. All authors read and approved the final manuscript.

Funding
This study was supported by the "Star of Jiaotong University" program of Shanghai Jiao Tong University Medical and the Industrial Cross Research Fund Project (grant no YG2019ZDB08) to Yuqing Chen.

Data availability
All data generated or analyzed during this study are included in this article.

Declarations

Ethics approval and consent to participate
This study does not involve humans and animals and is a purely mechanical simulation test with no ethical or consent required.

Consent for publication
Not applicable.

Competing interests
The authors declare no competing interests.

Received: 19 January 2024 / Accepted: 13 May 2024
Published online: 20 May 2024

References

1. Rittayamai N, Katsios CM, Beloncle F, Friedrich JO, Mancebo J, Brochard L. Pressure-controlled vs volume-controlled ventilation in Acute Respiratory failure: a physiology-based narrative and systematic review. Chest. 2015;148:340–55.
2. Şenay H, Sıvacı R, Kokulu S, Koca B, Bakı ED, Ela Y. The effect of pressure-controlled ventilation and volume-controlled ventilation in Prone position on pulmonary mechanics and inflammatory markers. Inflammation. 2016;39:1469–74.
3. Monjezi M, Jamaati H. The effects of pressure- versus volume-controlled ventilation on ventilator work of breathing. Biomed Eng Online. 2020;19:72.
4. Oğurlu M, Küçük M, Bilgin F, Sizlan A, Yanarateş O, Eksert S, et al. Pressure-controlled vs volume-controlled ventilation during laparoscopic gynecologic surgery. J Minim Invasive Gynecol. 2010;17:295–300.
5. Lee JM, Lee SK, Rhim CC, Seo KH, Han M, Kim SY, et al. Comparison of volume-controlled, pressure-controlled, and pressure-controlled volume-guaranteed ventilation during robot-assisted laparoscopic gynecologic surgery in the Trendelenburg position. Int J Med Sci. 2020;17:2728–34.
6. Thille AW, Cabello B, Galia F, Lyazidi A, Brochard L. Reduction of patient-ventilator asynchrony by reducing tidal volume during pressure-support ventilation. Intensive Care Med. 2008;34:1477–86.
7. Choi EM, Na S, Choi SH, An J, Rha KH, Oh YJ. Comparison of volume-controlled and pressure-controlled ventilation in steep Trendelenburg position for robot-assisted laparoscopic radical prostatectomy. J Clin Anesth. 2011;23:183–8.
8. Prella M, Feihl F, Domenighetti G. Effects of short-term pressure-controlled ventilation on gas exchange, airway pressures, and gas distribution in patients with acute lung injury/ARDS: comparison with volume-controlled ventilation. Chest. 2002;122:1382–8.
9. Ionescu C, Derom E, De Keyser R. Assessment of respiratory mechanical properties with constant-phase models in healthy and COPD lungs. Comput Methods Programs Biomed. 2010;97:78–85.
10. Arnal JM, Garnero A, Saoli M, Chatburn RL. Parameters for Simulation of adult subjects during mechanical ventilation. Respir Care. 2018;63:158–68.
11. Avanzolini G, Barbini P, Cappello A, Cevenini G, Chiari L. A new approach for tracking respiratory mechanical parameters in real-time. Ann Biomed Eng. 1997;25:154–63.
12. Hezarjaribi N, Dutta R, Xing T, Murdoch GK, Mazrouee S, Mortazavi BJ, et al. Monitoring lung mechanics during mechanical ventilation using machine learning algorithms. Annu Int Conf IEEE Eng Med Biol Soc. 2018;2018:1160–63.
13. Teggia-Droghi M, Grassi A, Rezoagli E, Pozzi M, Foti G, Patroniti N, et al. Comparison of two approaches to Estimate driving pressure during assisted ventilation. Am J Respir Crit Care Med. 2020;202:1595–98.
14. Pan Q, Pan J, Zhang Z, Fang L, Ge H. Assessment of respiratory system compliance under pressure control ventilation without an inspiratory pause maneuver. Physiol Meas. 2021;42.
15. Chen Y, Yuan Y, Zhang H, Li F, Wang X. Continuous estimation of airway resistance in non-invasive ventilation. Respir Physiol Neurobiol. 2021;294:103738.
16. Iotti GA, Braschi A, Brunner JX, Smits T, Olivei M, Palo A, et al. Respiratory mechanics by least squares fitting in mechanically ventilated patients: applications during paralysis and during pressure support ventilation. Intensive Care Med. 1995;21:406–13.
17. Peslin R, da Silva JF, Chabot F, Duvivier C. Respiratory mechanics studied by multiple linear regression in unsedated ventilated patients. Eur Respir J. 1992;5:871–8.
18. Volta CA, Marangoni E, Alvisi V, Capuzzo M, Ragazzi R, Pavanelli L, et al. Respiratory mechanics by least squares fitting in mechanically ventilated patients: application on flow-limited COPD patients. Intensive Care Med. 2002;28:48–52.
19. Vicario F, Albanese A, Karamolegkos N, Wang D, Seiver A, Chbat NW. Non-invasive estimation of respiratory mechanics in spontaneously breathing ventilated patients: a constrained optimization Approach. IEEE Trans Biomed Eng. 2016;63:775–87.
20. Nassar BS, Collett ND, Schmidt GA. The flow-time waveform predicts respiratory system resistance and compliance. J Crit Care. 2012;27:e4187–14.
21. Lopez-Navas K, Brandt S, Strutz M, Gehring H, Wenkebach U. Non-invasive determination of respiratory effort in spontaneous breathing and support ventilation: a validation study with healthy volunteers. Biomed Tech (Berl). 2014;59:335–41.
22. Becher TH, Bui S, Zick G, Bläser D, Schädler D, Weiler N, et al. Assessment of respiratory system compliance with electrical impedance tomography using a positive end-expiratory pressure wave maneuver during pressure support ventilation: a pilot clinical study. Crit Care. 2014;18:679.
23. Perchiazzi G, Rylander C, Pellegrini M, Larsson A, Hedenstierna G. Robustness of two different methods of monitoring respiratory system compliance during mechanical ventilation. Med Biol Eng Comput. 2017;55:1819–28.
24. Čandik P, Rybár D, Depta F, Sabol F, Kolesár A, Galková K, et al. Relationship between dynamic expiratory time constant tau(edyn) and parameters of breathing cycle in pressure support ventilation mode. Physiol Res. 2018;67:875–79.
25. Lichtwarck-Aschoff M, Kessler V, Sjöstrand UH, Hedlund A, Mols G, Rubertsson S, et al. Static versus dynamic respiratory mechanics for setting the ventilator. Br J Anaesth. 2000;85:577–86.
26. Chen Y, Yuan Y, Zhang H, Li F, Zhou X. Accuracy of the dynamic signal analysis approach in respiratory mechanics during noninvasive pressure support ventilation: a bench study. J Int Med Res. 2021;49:300060521992184.
27. Beloncle F, Akoumianaki E, Rittayamai N, Lyazidi A, Brochard L. Accuracy of delivered airway pressure and work of breathing estimation during proportional assist ventilation: a bench study. Ann Intensive Care. 2016;6:30.
28. Paredi P, Goldman M, Alamen A, Ausin P, Usmani OS, Pride NB, et al. Comparison of inspiratory and expiratory resistance and reactance in patients with asthma and chronic obstructive pulmonary disease. Thorax. 2010;65:263–7.
29. Sugiyama A, Hattori N, Haruta Y, Nakamura I, Nakagawa M, Miyamoto S, et al. Characteristics of inspiratory and expiratory reactance in interstitial lung disease. Respir Med. 2013;107:875–82.
30. Brunner JX, Laubscher TP, Banner MJ, Iotti G, Braschi A. Simple method to measure total expiratory time constant based on the passive expiratory flow-volume curve. Crit Care Med. 1995;23:1117–22.
31. Macklem PT. The mechanics of breathing. Am J Respir Crit Care Med. 1998;157:S88–94.
32. Barberis L, Manno E, Guérin C. Effect of end-inspiratory pause duration on plateau pressure in mechanically ventilated patients. Intensive Care Med. 2003;29:130–4.
33. Lucangelo U, Bernabé F, Blanch L. Respiratory mechanics derived from signals in the ventilator circuit. Respir Care. 2005;50:55–65. discussion 65 – 7.
34. Magalhães P, Padilha G, Moraes L, Santos CL, de Andrade LB, Magalhães M, et al. Effects of pressure-support ventilation with different levels of positive end-expiratory in a mild model of acute respiratory distress syndrome. Intensive Care Med Exp. 2015;3:A573.
35. Khirani S, Polese G, Aliverti A, Appendini L, Nucci G, Pedotti A, et al. On-line monitoring of lung mechanics during spontaneous breathing: a physiological study. Respir Med. 2010;104:463–71.
36. CJSo. Relation of volume history of lungs to respiratory mechanics in anesthetized dogs. Anesthesiology. 1959;5:669–78.

Publisher's Note